Experimental studies of the dangling- and dimer-bond-related surface electron bands on Si(100) (2×1)

R. I. G. Uhrberg, G. V. Hansson, J. M. Nicholls, and S. A. Flodström

Department of Physics and Measurement Technology, Linköping University, S-581 83 Linköping, Sweden

(Received 4 May 1981)

Angle-resolved ultraviolet photoelectron spectroscopy has been used to determine the initial-state energy versus $\vec{k}_{\parallel}$ dispersion of surface states on the Si(100) (2×1), two-domain, reconstructed surface. One surface state was found at 0.70 eV below E_F at the Γ symmetry point. The energy dispersion relation for this surface state was measured along the $\Gamma-J$, $\Gamma-J'$, and $J-K$ symmetry lines of the (2×1) surface Brillouin zone (SBZ). A second surface state was observed in the energy range between 2 and 3 eV below E_F. The energy dispersion relation for this surface state was obtained along the $J-K$ symmetry line of the SBZ and in the [010] bulk azimuthal direction. The experimentally obtained dispersion relations are compared with the surface electron bands as given by a tight-binding calculation of the asymmetric dimer model. The experiment gives a surface-state band whose center of gravity is in good agreement with the calculation, while the bandwidth is approximately half as large as the calculated. For the lower surface state both initial energy position and dispersion are in good agreement with the calculation. The upper surface state is assigned to a dangling-bond band and the lower is tentatively assigned to the dimer bond.

I. INTRODUCTION

The ideal Si(100) surface has two broken covalent bonds (dangling bonds) per surface atom. Since this situation is not energetically favorable, the surface reconstructs in order to lower its energy. The reconstruction of the Si(100) surface was first observed by Farnsworth and Schlier using low-energy-electron diffraction (LEED).[1] They observed a LEED pattern which could be explained by a doubling of the surface unit cell in one direction, this doubling being induced by the reconstruction. The actually observed LEED patterns are complicated by the different domains present on the Si(100) surface. One lattice step changes the direction of the long axis of the surface unit cell by 90°. The observed LEED pattern thus represents a superposition of two- (2×1) domain diffraction patterns. The (2×1) two-domain reconstruction is the most commonly reported reconstruction of the Si(100) surface.

A few groups have reported a $c(4\times2)$ reconstruction seen in LEED experiments.[2-4] The $c(4\times2)$ reconstruction, as well as (2×2) reconstructions, have also been found from He beam diffraction experiments on the Si(100) surface.[5]

Many different structural models have been suggested to account for the surface reconstructions. The models can be divided into chain models,[6,7] vacancy models,[3,8,9] and pairing (dimer) models.[1,10-12] Surface electronic band calculations have been performed on the basis of various suggested models.[13,14] The surface electron bands of the pairing model (symmetric)[14] are found to give the best agreement when compared to angular integrated photoemission data.[15] However, all three models give metallic surface bands, which is in disagreement with photoemission results.[15,16] An asymmetric dimer model has recently been suggested.[12] By making the dimer slightly ionic the surface energy will be lowered. The electronic surface band calculations[12,17] in this model display semiconducting surface bands in agreement with experimental data.

We have studied electronic structure using angle-resolved photoelectron spectroscopy (AR-UPS). LEED has been used to characterize the symmetry of the surfaces investigated. In Sec. III we present experimental dispersion relations $E_i(\vec{k}_{\parallel})$ (initial-state energy versus electron parallel momentum) for two surface-state structures. One surface-state structure is situated near the Fermi level (E_F) (Refs. 15 and 16) and the other structure is found

in the region between 2 and 3 eV below E_F. In Sec. IV the experimental data are directly compared with theoretical calculations of the surface electron bands.[12,17] In this paper we denote the states in the surface electron bands as surface states although they sometimes are actual surface resonances. We assign the upper surface state to a dangling-bond band and the lower state tentatively to the dimer bond.

II. EXPERIMENTAL DETAILS

Angular-resolved photoemission spectra were measured in an UHV chamber at a pressure of 1×10^{-10} Torr. The photoelectrons were excited using the monochromatized radiation from a hydrogen discharge. Useful photon energies were obtained in the range 7.0—11.6 eV. The emitted electrons were energy analyzed by a 180° spherical deflection analyzer rotatable in the plane of light incidence. Slit widths of the analyzer and analyzer radius were chosen to give a resolution $(\Delta E / E)$ of 1.5%.[19] Monochromator slits and analyzer voltages were set to obtain a combined energy resolution of ≤ 0.3 eV in the recorded spectra.

The sample was a Si(100) single-crystal boron doped to 8—12 Ω cm. It was cleaned in situ by repeated cycles of argon-ion bombardment (1000 V, 10 μA). Annealing at 800 °C for 5 min produced a sharp (2×1) two-domain LEED pattern. During the final annealing the pressure never rose above 2×10^{-9} Torr. The Fermi-level reference was obtained by photoelectron emission from the tantalum sample holder to an accuracy of ± 0.05 eV.

III. EXPERIMENTAL RESULTS

In Fig. 1 we show angle-resolved photoemission spectra for the Si(100) (2×1) reconstructed surface measured in the normal direction for photon energies between 8.6 and 11.6 eV. Structures B, C, D, and E show a clear dispersion in initial-state energy with photon energy, and we interpret them as due to direct interband transitions. These structures will not be further discussed in this paper.[20] Structure A does not show any initial-state dispersion with varying photon energy. Its position in initial-state energy is 0.70 eV below the Fermi level (E_F). There is a small shift of the peak position for $\hbar\omega = 9.4$ eV, which is induced by the bulk structure B which is moving towards the Fermi level for decreasing photon energies. The A peak is
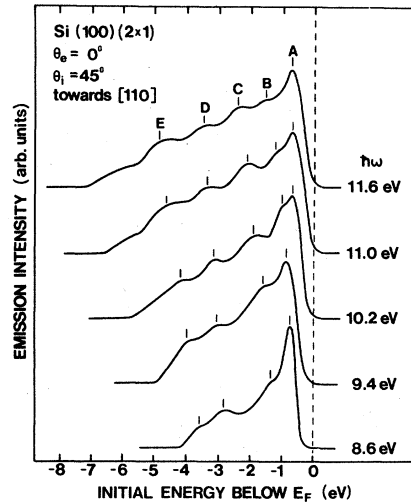
FIG. 1. Angle-resolved photoemission spectra, normal emission $(\theta_e = 0°)$, for photon energies from 8.6 to 11.6 eV.

sensitive to oxygen exposure, after 150-L O_2 exposure the emission is negligible (Fig. 2). The observed (2×1) two-domain LEED pattern remains sharp after this exposure and the structures assigned to bulk transitions are not strongly affected. We interpret peak A as due to surface-state emission. Peak A fulfills two of the criteria ascribed to surface states: no initial-state dispersion with photon energy for normal electron emission and extreme sensitivity to gas (oxygen) exposure. This surface state has been reported earlier.[15,16,18] The A
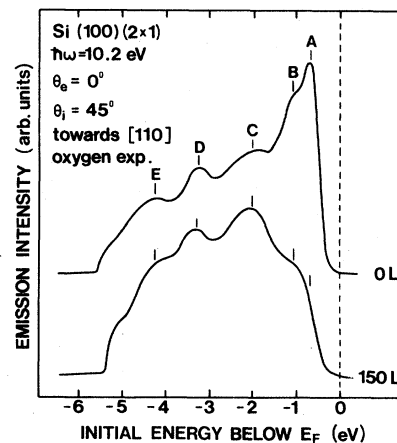
FIG. 2. Effect of oxygen exposure on the A surface-state emission.
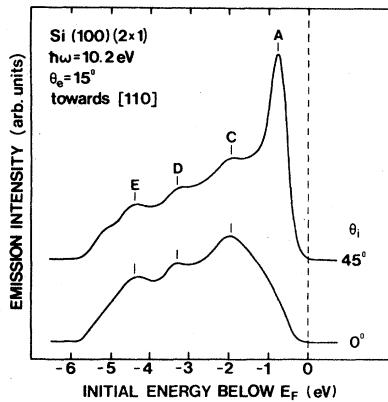
FIG. 3. Dependence of the A surface-state emission on the angle of light incidence. For normal light incidence $(\theta_i = 0°)$, the vector potential has no component normal to the surface.

surface-state emission also shows a strong dependence on polarization of the incident light. When varying the angle of light incidence to normal incidence, which makes the p-polarized component of the light disappear, we see very little emission from this surface state (Fig. 3).
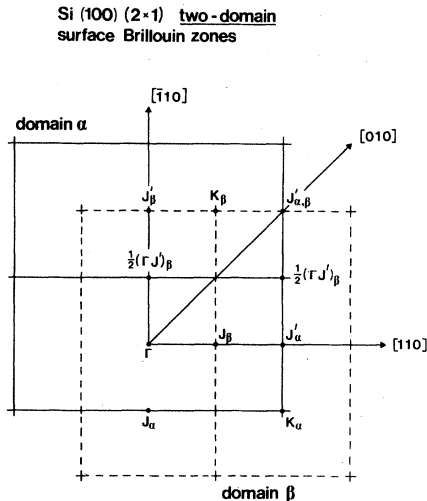
FIG. 4. Superposed surface Brillouin zones (SBZ) in the repeated zone scheme of the two (2×1) reconstructed domains of the Si(100) surface. The symmetry points of the (2×1) SBZ's are poined out, with indices identifying them with domain α and domain β, respectively. The bulk azimuthal directions are also indicated.

The energy versus $\vec{k}_{||}$ dispersion for the surface state was measured in the [110], [010], and [$\bar{1}$10] bulk azimuthal directions for $\hbar\omega = 10.2$ eV. As we observe a (2×1) *two-domain* pattern in LEED, we have to consider contributions to the photoemission spectra from *both domains*. Each domain will provide a (2×1) surface Brillouin zone (SBZ), but as the domains are rotated 90° with respect to each
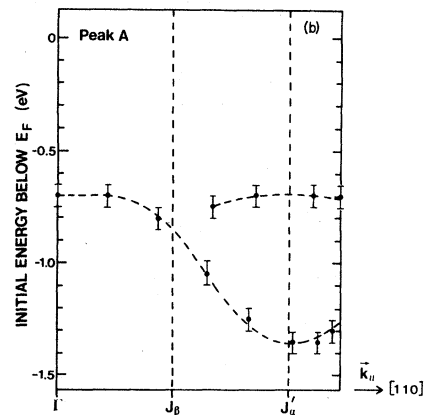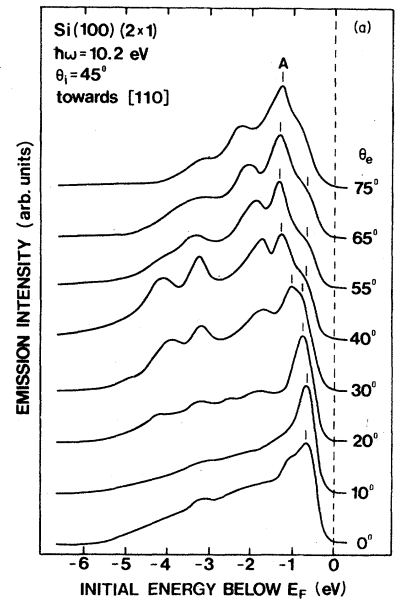
FIG. 5 (a). Angle-resolved photoemission spectra for different angles of electron emission. $\vec{k}_{||}$ for the emitted electrons is directed along the [110] azimuthal direction. (b) Initial energy vs $\vec{k}_{||}$ dispersion along the [110] azimuthal direction for peak A. The symmetry points J_β and J_α' of the two domains are indicated. The points at ~ 0.7 eV near J_α' correspond to the shoulder for $\theta_e \geq 30°$ in (a).

other, we obtain the final SBZ configuration as shown in Fig. 4. The [110], [010], and [$\bar{1}$10] directions have been indicated in the figure, these directions refer to the underlying three-dimensional bulk unit cell.

Photoemission spectra for different angles of emission (θ_e) in the [110] azimuthal direction are shown in Fig. 5(a). The surface state (A) at 0.70 eV below E_F for $\theta_e = 0°$ disperses downwards in initial-state energy to 1.35 eV below E_F for $\theta_e = 55°$ ($k_{||} \sim 0.84$ Å^{-1}), which corresponds to the J'_α symmetry point ($k_{||} \sim 0.82$ Å^{-1}). In calculating $k_{||}$ we have used the value of 4.85 eV for the work function.[15] For electron emission angles $\geq 30°$ we see a shoulder at approximately the same initial-state energy as the A peak for $\theta_e = 0°$. The initial-state energy versus $\vec{k}_{||}$ dispersion has been plotted in Fig. 5(b), where the symmetry points J_β and J'_α are indicated. In the [$\bar{1}$10] direction, that is rotating the crystal 90°, we measure the same dispersion for the A peak and we also see a shoulder coming up for emission angles $\geq 30°$.

The interpretation of the observed dispersions along the [110] and [$\bar{1}$10] directions is that the peak dispersing from 0.70 eV down to 1.35 eV below E_F corresponds to the A surface-state dispersion along the $\Gamma - J'$ line in the SBZ. When probing the $\Gamma - J'_\alpha$ direction in one Brillouin zone (domain α) we also probe the $\Gamma - J_\beta - \Gamma_\beta$ direction in the 90° rotated zone (domain β). The shoulder at 0.70 eV below E_F at angles $\geq 30°$ can be explained as emission from the $\Gamma - J_\beta - \Gamma_\beta$ direction in this rotated zone moved in emission angle by a surface umklapp process. The relative intensities of the dispersing peak and the shoulder are not the same for the [110] and [$\bar{1}$10] directions. The weak shoulder at 0.70 eV below E_F in emission form the [110] direction become more like a peak in the [$\bar{1}$10] direction, while the emission from the dispersed peak is reduced in this direction. An explanation to this intensity variation is that we do not have equal amounts of the two domains in the surface.

The surface-state dispersion has also been measured in the [010] direction in order to eliminate the ambiguity due to superposition of the two surface Brillouin zones (Fig. 4). The photoemission spectra and measured dispersion for the A peak in this direction are shown in Fig. 6. Using $\hbar\omega = 10.2$ eV, we could not reach the $J'_{\alpha,\beta}$ point in the repeated zone scheme along the [010] direction. We measured the dispersion up to $\theta_e = 70°$, which corresponds to ~ 0.84 of the $\Gamma - J'_{\alpha,\beta}$ distance. For

$\theta_e \geq 50°$ we observe a peak (F) at 0.85 eV below E_F, that is approximately the same energy as for the surface state at Γ. In the [010] direction we probe equivalent $\vec{k}_{||}$ points in both Brillouin zones, and this extra peak cannot be explained by the sur-
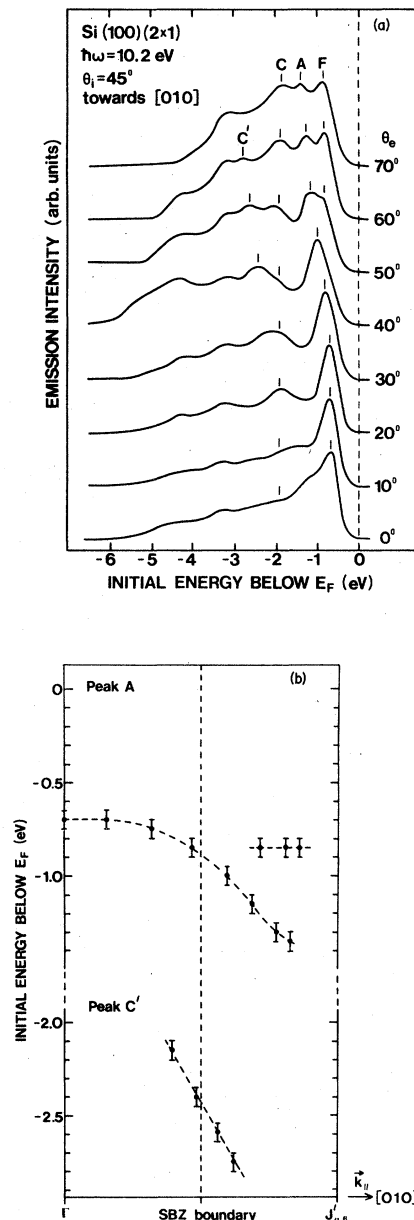
FIG. 6 (a) Angle-resolved photoemission spectra for different angles of electron emission. $\vec{k}_{||}$ for the emitted electrons is directed along the [010] azimuthal direction. (b) Initial energy vs $\vec{k}_{||}$ dispersion along the [010] azimuthal direction for both the A and C' surface states.

face umklapp process suggested for the [110] and [$\bar{1}$10] directions. In Fig. 6(a) we see an additional surface related structure (C') for initial-state energies between 2 and 3 eV below E_F. This structure is not seen in the [110] or [$\bar{1}$10] directions. For $\theta_e = 30°$ we see a broadening of the bulk structure observed at 2.0 eV below E_F in the $\theta_e = 0°$ spectra (C in Fig. 1). For $\theta_e = 40°$ we see an asymmetric peak at 2.5 eV below E_F, indicating contribution from two different peaks. For $\theta_e = 50°$ and 60° we clearly see that this additional surface peak has split off from the original bulk peak and is dispersing downwards in energy with increasing angles of electron emission, while the original bulk peak shows no dispersion in θ_e.

To check the surface character of the C' peak we cannot use the criterion that no initial-state energy versus photon energy dispersion should be observed for surfaces states in the normal emission spectra, simply because the C' peak cannot be detected there.

In Fig. 7 we display spectra taken in the [010] azimuthal direction at $\theta_e = 55°$ for different oxygen exposures. The position of the C' peak for the clean surface is 2.45 eV below E_F. We also see a shoulder at 2.0 eV below E_F, which is the C bulk peak. For increasing oxygen exposures we observed how the emission intensity of the 2.45-eV peak (C') decreases, and at 400-L O_2 exposure the remaining

structure observed is the 2.0-eV (C) peak. The A surface-state peak at ~ 1 eV below E_F has also disappeared at 400-L O_2 exposure. After 400-L O_2 exposure we could still detect a two-domain (2×1) LEED pattern, but diffuse compared to the original "clean" one. From the oxygen exposure data we interpret the C' peak as being due to emission from a surface state. The initial-state energy versus $\vec{k}_{||}$ dispersion for the C' surface state is shown in Fig. 6(b) for the [010] azimuthal direction. In Fig. 8 the dependence on light polarization is displayed, and we see that for normal light incidence both the A surface-state and the C' surface-state emission are reduced.

By choosing the azimuthal and the polar angle of electron emission we can probe $\vec{k}_{||}$ points at (or very close to) the $J - K$ symmetry line in the surface Brillouin zone, but we still have the ambiguity due to the two superimposed (2×1) domains. In the experimental data the C' surface state is only observed for $\vec{k}_{||}$ points being closer to the K than to the J symmetry point. When varying $\vec{k}_{||}$ from K to J, the C' surface state moves closer to the bulk state (C) at 2.0 eV below E_F, and for $\vec{k}_{||}$ points close to J we cannot separate the two different contributions.

The $J_\alpha - K_\alpha$ symmetry line in the surface Brillouin zone for domain α corresponds to a line through the $\frac{1}{2}$ $\Gamma J'_\beta$ point and perpendicular to the $\Gamma - J'_\beta$ line in the surface Brillouin zone for the 90° rotated domain (domain β). $\vec{k}_{||}$ points close to J_α corresponds to $k_{||}$ close to $\frac{1}{2}$ $\Gamma J'_\beta$ in the 1st SBZ,

FIG. 7. Effect of oxygen exposure on the A and C' surface-state emission.
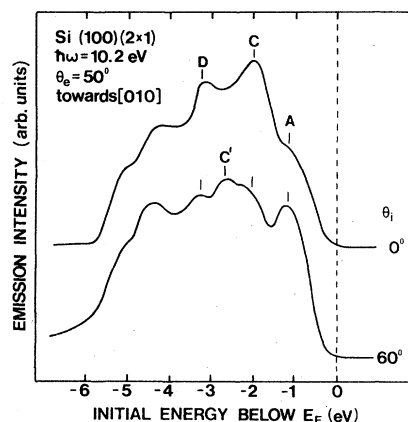
FIG. 8. Dependence of the A and C' surface-state emission on the angle of light incidence.

and $\vec{k}_{||}$ points close to K_α corresponds to $\vec{k}_{||}$ points close to $\frac{1}{2}\Gamma J_\beta'$ in the 2nd SBZ (repeated zone scheme) in the rotated domain. Since the C' surface state was observed for $\vec{k}_{||}$ points close to K_α, i.e., close to $\frac{1}{2}\Gamma J_\beta'$ in the 2nd SBZ in domain β we would expect to observe the C' surface state close to $\frac{1}{2}\Gamma J_\beta'$ in the 1st SBZ if we tried to interpret the data in the surface Brillouin zone of domain β. However, since this point is the J_α point in domain α, where we cannot observe the C' surface state, any interpretation using the rotated domain (β) can be ruled out. The observed initial energy versus $\vec{k}_{||}$ dispersion is thus taken as the *actual* dispersion along the $J-K$ symmetry line.

IV. DISCUSSION

The (2×1) LEED pattern is the most frequently observed diffraction pattern from the Si(100) surface. Additional quarter-order diffraction spots indicating a $c(4\times2)$ reconstruction have been observed in LEED by a few groups.[2-4]. He beam diffraction experiments by Cardillo and Becker[5] have shown diffuse diffraction beams which are consistent with the existence of $c(4\times2)$, $p(2\times2)$, and $c(2\times2)$ reconstructed domains of the Si(100) surface. In our LEED experiments we did not observe any diffraction spots or streaks indicating a $c(4\times2)$ or any (2×2) reconstructions. The diffraction pattern was observed with the naked eye for various kinetic energies (50—200 eV) of the incident electrons. The discussion of the experimental angle-resolved photoemission results will thus be done within the frame of the (2×1) reconstructed Si(100) surface. The minima of the energy dispersions for the surface state A in the [110] and [$\bar{1}$10] azimuthal directions are at the J' symmetry point (Fig. 4), which is expected for the (2×1) surface reconstruction.

One of the most common models for the (2×1) reconstruction of the Si(100) surface is the dimer model suggested by Schlier and Farnsworth.[1] This symmetric dimer model can be further manipulated. By tilting the dimer bond and allowing for a charge transfer between the two atoms participating in the dimer bond, a surface reconstruction of lower total energy than the symmetric dimer can be obtained.[12] Surface band calculations for the asymmetric dimer gives semiconducting surface bands, contrary to the symmetric dimer. The semiconducting surface bands are consistent with the
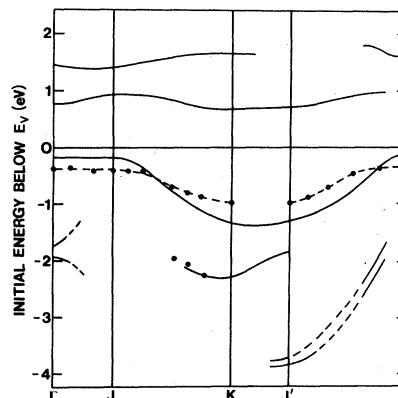
FIG. 9. Comparison between the experimentally obtained surface-state bands (filled circles) and theoretical bands as given by a TB calculation for the asymmetric dimer model (Ref. 12).

present and earlier reported photoemission experiments.[15,16,18]

In Fig. 9 we have plotted the experimentally obtained initial energy dispersion of the surface states A and C' along the different symmetry lines in the (2×1) SBZ. The shoulder near the Fermi level observed in the [110] and [$\bar{1}$10] directions for emission angles $\geq 30°$ has been plotted along the $\Gamma-J$ line according to the interpretation suggested in Sec. III. In Fig. 9 we have also plotted the surface-state bands as given by a tight-binding (TB) calculation for the asymmetric dimer model.[12]

The A peak is identified as the dangling-bond surface state.[16] We suggest that the C' peak can be identified as the "bridge-bond" surface state, i.e., a surface state induced by the covalent bond in the surface plane between the atoms forming the dimer. For the symmetric dimer Appelbaum *et al.*[14] found a peak in the calculated local density of states for the bridge bond at 2.5 eV below E_v. For the asymmetric dimer model, a pseudopotential calculation by Ihm *et al.*[17] showed a bridge-bond surface resonance at 2.2 eV below E_v at the K symmetry point.

Qualitatively the agreement between the observed and calculated surface bands for the dangling-bond state (A) is quite good. The absence of dispersion along the $\Gamma-J$ symmetry line and the general shape of the dispersions along the $J-K$ and $\Gamma-J'$ symmetry lines deduced from the experiments, agrees well with corresponding features in the calculation. The center of gravity of

the calculated dangling-bond band is in good agreement with our experiment, while the bandwidth is twice as large. The calculated bandwidth for the $\Gamma - J'$ symmetry line is 1.2 eV, while the experimental bandwidth is 0.65 eV. Earlier experiments have reported a bandwidth of 0.5 eV.[16] The experimental initial energy for the dangling-bond state is ~ 0.40 eV below E_v,[21] while the calculated value is 0.12 eV below E_v.[12] Pseudopotential calculations.[17] give a better value for the bandwidth, but place the dangling-bond band too high in energy. For the lower surface state C' we find that both the dispersion along the $J - K$ line and its energy position are in good agreement with the corresponding surface-state band in the calculation. It should be noted that in the TB calculation no identification of the calculated C' surface state with the dimer bond is made.[12,22]

The asymmetric dimer-model gives only *one* filled surface-state band near the valence-band maximum; which is *not consistent* with the experimentally observed additional peak at 0.85 eV below E_F in the [010] azimuthal direction. A possible explanation to this peak in terms of the presence of additional domains of other reconstructions on the Si(100) surface has been suggested, e.g., $c(4\times2)$, $c(2\times2)$, $p(2\times2)$. Both the $c(4\times2)$ and the two (2×2) reconstructions can qualitatively explain the existence of the additional peak. A (2×2) reconstruction provides a surface reciprocal-lattice vector which takes the J' point into the Γ point of the 1st SBZ. The additional peak at 0.85 eV below E_F for $\theta_e \geq 50°$ (Fig.6) can thus be explained as emission from $\vec{k}_{||}$ points along the [010] direction inside the 1st SBZ that have been moved in emission angle by a surface reciprocal-lattice vector of the (2×2) reconstruction. The C' surface state crosses

the 1st SBZ boundary along the [010] direction at $\theta_e = 42°$. With a (2×2) reconstructed domain present, we would expect to observe in our spectra a peak for $\theta_e \geq 50°$ associated with emission from the C' surface state for $\vec{k}_{||}$ points inside the 1st SBZ. Since the C' surface state is very close (or degenerate) in initial-state energy with the C bulk state for $\vec{k}_{||}$ "inside" the 1st SBZ , we cannot judge from our spectra if this surface umklapp process is present as suggested for the A surface state.

V. SUMMARY

We have found that the general shape of the experimentally obtained initial energy dispersion, of the dangling-bond surface state is in good agreement with a TB calculation for the asymmetric dimer model along the symmetry lines of the (2×1) reconstructed SBZ. The bandwidth is, however, 50% smaller than in this calculation. The additional peak at 0.85 eV below E_F for the [010] azimuthal direction cannot be explained in terms of the dangling-bond surface state for the (2×1) reconstruction.

The TB calculation also gives a surface-state band, whose energy position is in good agreement with the observed C' surface state for $\vec{k}_{||}$ close to the K symmetry point. A surface band calculation for the $c(4\times2)$ reconstruction by the same author[12] does not give the same good agreement for the C' surface state.

Note added in proof. The calculated surface state at 2.3 eV near the K point (Ref. 12) is predominantly a p_z character orbital on second-layer atoms on the chain that contains the lowered atom of the surface dimer. About $\frac{1}{5}$ of its character is p_y from the lowered atom of the dimer.[22]

[1]R. E. Schlier and H. E. Farnsworth, J. Chem. Phys. 30, 917 (1959).

[2]J. J. Lander and J. Morrison, J. Chem. Phys. 37, 729 (1962).

[3]T. D. Poppendieck, T. C. Ngoc, and M. B. Webb, Surf. Sci. 75, 287 (1978).

[4]P. M. Gundry, R. Holtom, and V. Leverett, Surf. Sci. 43, 647 (1974).

[5]M. J. Cardillo and G. E. Becker, Phys. Rev. Lett. 40, 1148 (1978); Phys. Rev. B 21, 1497 (1980).

[6]F. Jona, H. B. Shih, A. Ignatiev, D. W. Jepsen, and P. M. Marcus, J. Phys. C 10, L67 (1977).

[7]R. Seiwatz, Surf. Sci. 2, 473 (1964).

[8]J. C. Phillips, Surf. Sci. 40, 459 (1973).

[9]W. A. Harrison, Surf. Sci. 55, 1 (1976).

[10]J. A. Appelbaum and D. R. Hamann, Surf. Sci. 74, 21 (1978).

[11]J. P. Levine, Surf. Sci. 34, 90 (1973).

[12]D. J. Chadi. Phys. Rev. Lett. 43, 43 (1979); J. Vac. Sci. Technol. 16, 1290 (1979).

[13]G. P. Kerker, S. G. Louie, and M. L. Cohen, Phys. Rev. B 17, 706 (1978).

[14]J. A. Appelbaum, G. A. Baraff, and D. R. Hamann, Phys. Rev. Lett. 35, 729 (1975); Phys. Rev. B 14, 588 (1976).

[15]J. E. Rowe, Phys. Lett. 46A, 400 (1974); Phys. Rev. Lett. 32, 421 (1974).

[16]F. J. Himpsel and D. E. Eastman, J. Vac. Sci. Tech-

nol. 16, 1297 (1979).

[17]J. Ihm, M. L. Cohen, and D. J. Chadi, Phys. Rev. B 21, 4592 (1980).

[18]J. E. Rowe and S. B. Christman, J. Vac. Sci. Technol. 17, 220 (1980).

[19]D. Roy and J.-D. Carette, Can. J. Phys. 49, 2138 (1971).

[20]R. I. G. Uhrberg et al. (unpublished).

[21]When comparing the experimental data with the calculations we have used $E_F - E_v = 0.35$ eV, see Ref. 16.

[22]J. Chadi (private communication).